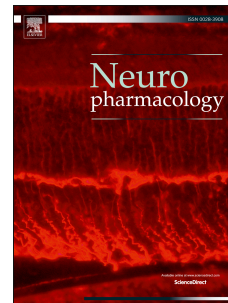


# Accepted Manuscript

The muscarinic antagonists scopolamine and atropine are competitive antagonists at 5-HT<sub>3</sub> receptors

Martin Lochner, Andrew J. Thompson



PII: S0028-3908(16)30167-8

DOI: [10.1016/j.neuropharm.2016.04.027](https://doi.org/10.1016/j.neuropharm.2016.04.027)

Reference: NP 6279

To appear in: *Neuropharmacology*

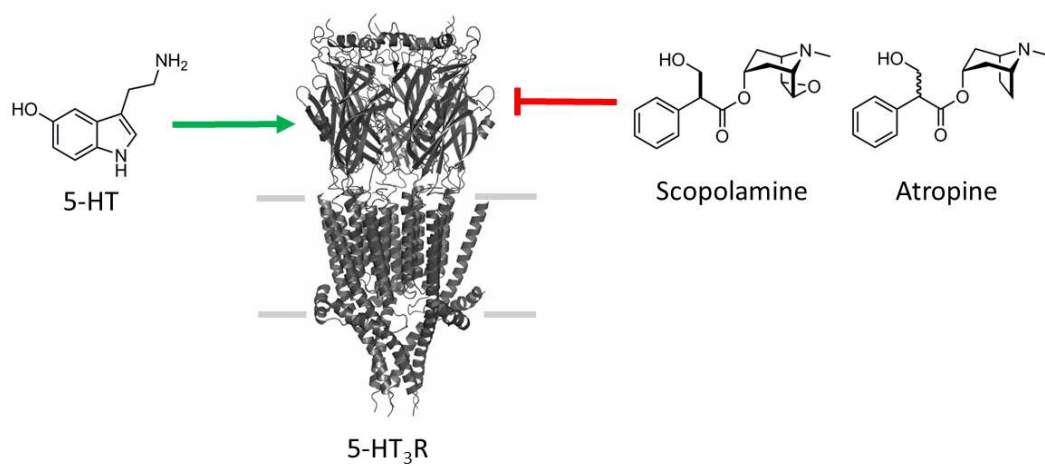
Received Date: 6 November 2015

Revised Date: 9 March 2016

Accepted Date: 20 April 2016

Please cite this article as: Lochner, M., Thompson, A.J., The muscarinic antagonists scopolamine and atropine are competitive antagonists at 5-HT<sub>3</sub> receptors, *Neuropharmacology* (2016), doi: 10.1016/j.neuropharm.2016.04.027.

This is a PDF file of an unedited manuscript that has been accepted for publication. As a service to our customers we are providing this early version of the manuscript. The manuscript will undergo copyediting, typesetting, and review of the resulting proof before it is published in its final form. Please note that during the production process errors may be discovered which could affect the content, and all legal disclaimers that apply to the journal pertain.



# The Muscarinic Antagonists Scopolamine and Atropine are Competitive Antagonists at 5-HT<sub>3</sub> Receptors.

*Martin Lochner<sup>1</sup> & Andrew J. Thompson<sup>2</sup>*

<sup>1</sup> Department of Chemistry and Biochemistry, University of Bern, Freiestrasse 3, CH-3012, Bern, Switzerland. Tel +41 31 631 4361. email: [martin.lochner@dcb.unibe.ch](mailto:martin.lochner@dcb.unibe.ch)

<sup>2</sup> Dr Andrew J. Thompson, Department of Pharmacology, Tennis Court Road, Cambridge CB2 1PD, UK. Tel: +44 1223 334000. email: [ajt44@cam.ac.uk](mailto:ajt44@cam.ac.uk)

**ABSTRACT**

Scopolamine is a high affinity muscarinic antagonist that is used for the prevention of post-operative nausea and vomiting. 5-HT<sub>3</sub> receptor antagonists are used for the same purpose and are structurally related to scopolamine. To examine whether 5-HT<sub>3</sub> receptors are affected by scopolamine we examined the effects of this drug on the electrophysiological and ligand binding properties of 5-HT<sub>3A</sub> receptors expressed in *Xenopus* oocytes and HEK293 cells, respectively. 5-HT<sub>3</sub> receptor-responses were reversibly inhibited by scopolamine with an  $IC_{50}$  of 2.09  $\mu$ M. Competitive antagonism was shown by Schild plot ( $pA_2 = 5.02$ ) and by competition with the 5-HT<sub>3</sub> receptor antagonists [<sup>3</sup>H]granisetron ( $K_i = 6.76 \mu$ M) and G-FL ( $K_i = 4.90 \mu$ M). The related molecule, atropine, similarly inhibited 5-HT evoked responses in oocytes with an  $IC_{50}$  of 1.74  $\mu$ M, and competed with G-FL with a  $K_i$  of 7.94  $\mu$ M. The reverse experiment revealed that granisetron also competitively bound to muscarinic receptors ( $K_i = 6.5 \mu$ M). In behavioural studies scopolamine is used to block muscarinic receptors and induce a cognitive deficit, and centrally administered concentrations can exceed the  $IC_{50}$  values found here. It is therefore possible that 5-HT<sub>3</sub> receptors are also inhibited. Studies that utilise higher concentrations of scopolamine should be mindful of these potential off-target effects.

## 1 INTRODUCTION

2 Scopolamine is a high-affinity (nM) muscarinic antagonist that is used to treat  
3 post-operative nausea and vomiting, and motion sickness. As a research tool it is often  
4 administered to induce cognitive dysfunction. At higher doses it can also produce  
5 amnesia and compliance (Klinkenberg and Blokland, 2010). Atropine is a related  
6 muscarinic antagonist from the same biosynthetic pathway as scopolamine and is used  
7 as a cycloplegic and mydriatic in ophthalmology, and for the treatment of  
8 bradychardia.

9 Scopolamine readily passes the blood brain barrier and it is believed that  
10 inhibition of muscarinic receptors in the central nervous system causes a cholinergic  
11 deficit that impairs memory (Klinkenberg and Blokland, 2010). As an age-related  
12 deterioration in cognitive function is thought to be predominantly related to a decline  
13 in cholinergic neurotransmission, scopolamine administration has often been used to  
14 model dementia (Bartus, 2000). Scopolamine has therefore been extensively used for  
15 preclinical and clinical testing of treatments for cognitive impairment (Bartolomeo et  
16 al., 2000; Blin et al., 2009; Liem-Moolenaar et al., 2011).

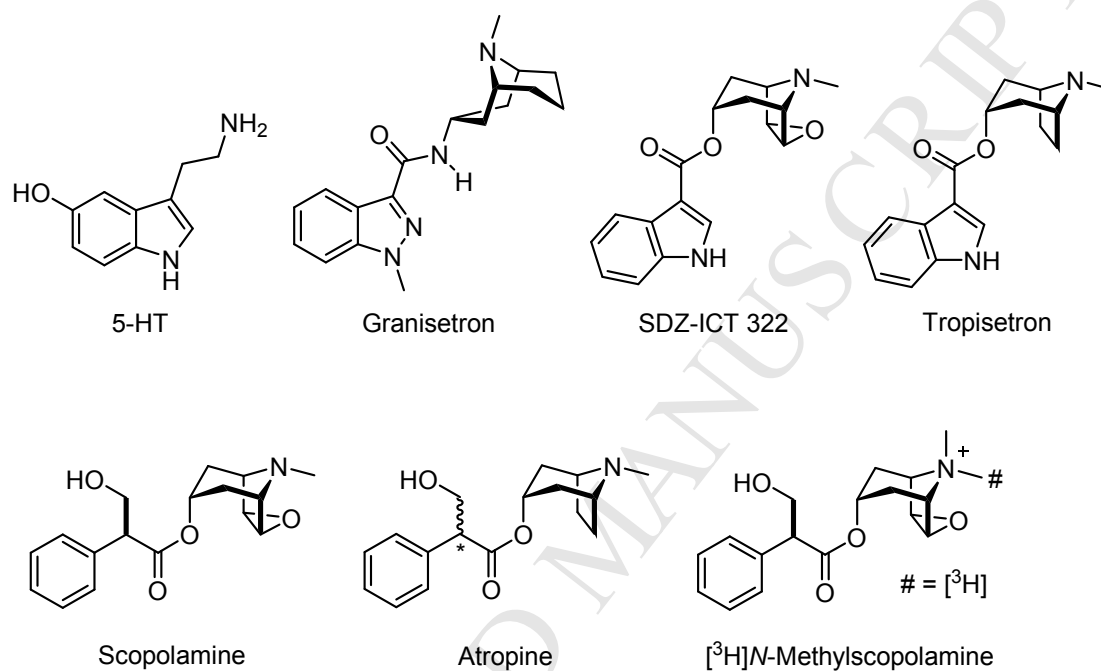
17 In the clinic, 5-HT<sub>3</sub> antagonists are mainly used for the treatment of nausea  
18 and vomiting following cancer therapy and general anaesthesia (Thompson 2013;  
19 Walstab *et al.*, 2010). Experimentally, they can also be administered to reverse  
20 scopolamine-evoked learning and memory deficits (Barnes et al., 1990; Chugh et al.,  
21 1991; Carli et al., 1997). In the brain 5-HT<sub>3</sub> receptors are widely distributed in the  
22 amygdala and hippocampus, regions of critical importance in memory and spatial  
23 navigation, and involved in the control of emotional responses and their associated  
24 disorders such as anxiety and depression (Gulyas et al., 1999; Thompson and  
25 Lummis, 2007; Walstab et al., 2010). It is thought that the reversal of scopolamine-

26 induced cognitive dysfunction by 5-HT<sub>3</sub> receptor antagonists occurs by inhibiting pre-  
27 synaptic 5-HT<sub>3</sub> receptors that modulate the functions of other neurotransmitters such  
28 as acetylcholine, dopamine,  $\gamma$ -aminobutyric acid and glutamate in this region  
29 (Seyedabadi et al., 2014). A similar mechanism is thought to underlie the anti-  
30 anxiolytic and anti-depressive actions of 5-HT<sub>3</sub> antagonists.

31 5-HT<sub>3</sub> receptors are members of the Cys-loop family of ligand-gated ion  
32 channels (LGIC). These are responsible for fast excitatory and inhibitory  
33 neurotransmission in the central and peripheral nervous systems. The family includes  
34 nicotinic acetylcholine (nACh),  $\gamma$ -aminobutyric acid (GABA<sub>A</sub>) and glycine  
35 receptors, which are all cell-surface, transmembrane ion channels. They consist of  
36 five subunits that surround a central ion-conducting pore, and each subunit contains  
37 three distinct functional regions that are referred to as the extracellular,  
38 transmembrane and intracellular domains. The orthosteric binding site (that occupied  
39 by the endogenous agonist) is located between the extracellular domains of adjacent  
40 subunits, and is formed by the convergence of three amino acid loops from the  
41 principal subunit (loops A - C) and three  $\beta$ -sheets (loops D - F) from the  
42 complementary subunit (Thompson et al., 2008). Agonist binding results in the  
43 opening of a central ion-conducting pore that is located within the transmembrane  
44 domain (Peters et al., 2010; Hassaine et al., 2014). Ligands bind to both domains, but  
45 the orthosteric binding site is the main drug target. These 5-HT<sub>3</sub> receptor competitive  
46 antagonists have high affinities (nM) and conform to a pharmacophore that consists of  
47 an aromatic group coupled to an azabicyclic ring via a carbonyl linker (fig 1). Both  
48 atropine and scopolamine also have these structural features, suggesting that these  
49 muscarinic antagonists could also bind at 5-HT<sub>3</sub> receptors (Thompson, 2013).

50 Here we use a combination of electrophysiology, radioligand binding, flow  
 51 cytometry and *in silico* ligand docking to provide evidence that, in addition to its  
 52 block of muscarinic receptors, scopolamine is also a competitive antagonist of 5-HT<sub>3</sub>  
 53 receptors.

54



57 **Figure 1**

58 Chemical structures of endogenous agonist 5-HT, 5-HT<sub>3</sub> receptor antagonists  
 59 granisetron, tropisetron and SDZ-ICT 322, scopolamine, atropine and the radioligand  
 60 [<sup>3</sup>H]N-methylscopolamine. Note that scopolamine is a single enantiomer whereas  
 61 atropine is a mixture of epimers at the indicated (asterisk) carbon atom.

62

## 63 MATERIALS AND METHODS

64 **Materials:** Atropine and scopolamine were from Sigma-Aldrich (St. Louis,  
 65 MO, USA). [<sup>3</sup>H]N-methylscopolamine (84 Ci/mmol) was from Perkin Elmer (Boston,

66 MA, USA). Human 5-HT<sub>3A</sub> (Accession: 46098) subunit cDNA was kindly provided  
67 by J. Peters (Dundee University, UK).

68 **Oocyte Maintenance:** *Xenopus laevis* oocytes were purchased from EcoCyte  
69 Bioscience (Castrop-Rauxel, Germany) and maintained according to standard  
70 methods (Goldin, 1992) in ND96 (96 mM NaCl, 2 mM KCl, 1 mM MgCl<sub>2</sub>, 5 mM  
71 HEPES, pH 7.4).

72 **Cell culture:** Human embryonic kidney (HEK) 293 cells were grown on 90  
73 mm round tissue culture plates as monolayers in DMEM / F12 (Gibco, Life  
74 Technologies, CA, USA) supplemented with 10% fetal bovine serum (FBS; Sigma  
75 Aldrich) at 37°C in a moist atmosphere containing 5% CO<sub>2</sub>.

76 **5-HT<sub>3</sub> Receptor Expression:** 5-HT<sub>3A</sub> subunit cDNA was cloned into  
77 pGEMHE for oocyte expression. cRNA was *in vitro* transcribed from linearised  
78 plasmid cDNA template using the mMessage mMachine Ultra T7 Transcription kit  
79 (Ambion, Austin, Texas, USA). Stage V and VI oocytes were injected with 50 nl of  
80 100-600 ng / µl cRNA (5 - 25 ng injected), and currents were recorded 1 - 3 days  
81 post-injection.

82 5-HT<sub>3A</sub> subunit cDNA was cloned into pcDNA3.1 for expression in HEK 293  
83 cells. Cells were transiently transfected with this cDNA using polyethyleneimine  
84 (PEI: 25 kDa, linear, powder, Polysciences Inc., Eppelheim, Germany). 30 µl of PEI  
85 (1 mg ml<sup>-1</sup>), 5 µl cDNA and 1 ml DMEM were incubated for 10 min at room  
86 temperature, added drop wise to a 90mm plate, at 80 - 90% confluency, and incubated  
87 for 2–3 days before harvesting.

88 **Muscarinic Receptor Preparation:** Muscarinic receptors were isolated from  
89 the cerebral cortices of adult male Guinea pigs (200-300 g). Brains were dissected  
90 into 10 mM Tris-HCl + 1 mM EDTA (pH 7.6) on ice and homogenised using a



91 Teflon-glass homogeniser with a motor-driven pestle (30 s, 300 rpm). The tissue was  
92 pelleted 17,000 g for 30 min and the membranes resuspended, and then centrifuged  
93 again using the same procedure. The final pellet was homogenised in 10 mM HEPES  
94 buffer (pH 7.4) and used directly for radioligand binding. Experiments involving  
95 animals were approved by the University of Cambridge Animal Welfare and Ethical  
96 Review Body (PHARM 004/15).

97 **Radioligand Binding:** Saturation binding (8 point) curves were measured by  
98 incubating either crude extracts of HEK 293 cells stably expressing 5-HT<sub>3</sub> receptors,  
99 or Guinea pig membrane preparations, in 0.5 ml incubations containing 10 mM  
100 HEPES buffer (pH 7.4) and 0.1 – 1 nM [<sup>3</sup>H]granisetron or 1 – 10 nM [<sup>3</sup>H]*N*-  
101 methylscopolamine. Competition binding (10 point) was determined by incubating the  
102 same receptors preparations in 0.5 ml HEPES buffer containing either 0.6 nM  
103 [<sup>3</sup>H]granisetron or 0.6 nM [<sup>3</sup>H]*N*-methylscopolamine, and differing concentrations of  
104 competing ligands. Non-specific binding was determined with 1 mM quipazine or 10  
105 μM scopolamine respectively. Incubations were terminated by filtration onto  
106 Whatman GF / B filters (Sigma Aldrich) wetted with HEPES buffer + 0.3 %  
107 polyethyleneimine, followed by two rapid washes with ice-cold HEPES buffer.  
108 Protein concentration was calculated using a Lowry protein assay with bovine serum  
109 albumin standards (Lowry et al., 1951). Radioactivity was measured using a Tri-Carb  
110 2100TR (Perkin Elmer, Waltham, MA, USA) scintillation counter.

111 **Flow Cytometry:** HEK 293 cells expressing the 5-HT<sub>3</sub> receptor were grown in  
112 monolayers and harvested from 90 mm culture dishes using 10 ml Trypsin-EDTA  
113 (Sigma Aldrich) for 10 min at 37°C. Digestion was terminated by the addition of 25  
114 ml DMEM + 10% FBS and cells pelleted at low speed for 2 min. The pellet was  
115 resuspended in 3 ml phosphate buffered saline (PBS: 137 mM NaCl, 8.0 mM

116  $\text{Na}_2\text{HPO}_4$ , 2.7 mM KCl, 1.47 mM  $\text{KH}_2\text{PO}_4$ , pH 7.4) and cells filtered through a cell  
117 strainer (BD Falcon, Franklin Lakes, NJ, USA). Competition binding was measured  
118 by incubating HEK 293 cells with different concentrations of non-labeled ligands and  
119 10 nM G-FL (Jack et al., 2015; Lochner and Thompson, 2015). After 10 min  
120 incubation, cells were pelleted and rapidly washed in PBS before being resuspended  
121 in the same buffer and analysed on a BD Accuri C6 flow cytometer (Becton,  
122 Dickinson and Company, NJ, USA) at 488 nm excitation / 530 nm emission.

123 **Electrophysiology:** Using two electrode voltage clamp, *Xenopus* oocytes were  
124 routinely clamped at -60 mV using an OC-725 amplifier (Warner Instruments,  
125 Connecticut, USA), NI USB-6341 X Series DAQ Device (National Instruments,  
126 Berkshire, UK) and the Strathclyde Electrophysiology Software Package (University  
127 of Strathclyde, UK). Micro-electrodes were fabricated from borosilicate glass  
128 (GC120TF-10, Harvard Apparatus, Edenbridge, Kent, UK) using a two stage  
129 horizontal pull (P-1000, Sutter Instrument Company, California, USA) and filled with  
130 3 M KCl. Pipette resistances ranged from 0.7 - 1.5 M $\Omega$ . Oocytes were routinely  
131 perfused with ND96 at a rate of 15 ml min<sup>-1</sup>. Drug application was via a simple  
132 gravity fed system calibrated to run at the same rate. Antagonists were routinely co-  
133 applied in the presence of 2  $\mu\text{M}$  5-HT or continuously applied for 1 min before the co-  
134 application of 2  $\mu\text{M}$  5-HT. A 2 min wash was used between applications.

135 **Data Analysis:** All data analysis was performed with GraphPad Prism v5.00  
136 (GraphPad Software, San Diego, CA, USA). For concentration-response curves, peak  
137 currents were measured for each concentration of agonist and normalised to the peak  
138 current in the same oocyte. For inhibition curves, the peak current response to 2  $\mu\text{M}$   
139 5-HT was measured at in the absence or presence of antagonist and normalised to the  
140 response to 2  $\mu\text{M}$  5-HT alone. The mean and S.E.M. for a series of oocytes was

141 plotted against agonist or antagonist concentration and iteratively fitted to the  
 142 following equation:

$$143 \quad y = I_{\min} + \frac{I_{\max} - I_{\min}}{1 + 10^{\log(EC_{50} - x)^{n_H}}} \quad (Equ. 1)$$

145 where  $I_{\min}$  is the baseline current,  $I_{\max}$  is the peak current evoked by agonist,  $EC_{50}$  is  
 146 the concentration of agonist needed to evoke a half-maximal response,  $x$  is the ligand  
 147 concentration and  $n_H$  is the Hill slope.  $K_b$  was estimated from  $IC_{50}$  values using the  
 148 Cheng-Prusoff equation with the modification by Leff and Dougall (1993):((Leff and  
 149 Dougall, 1993)

$$150 \quad K_b = \frac{IC_{50}}{((2 + ([A]/[A_{50}])^{n_H})^{1/n_H}) - 1} \quad (Equ. 2)$$

151 where  $K_b$  is the dissociation constant of the competing drug,  $IC_{50}$  is the concentration  
 152 of antagonist required to half the maximal response,  $[A]$  is the agonist concentration,  
 153  $[A_{50}]$  is the agonist  $EC_{50}$ , and  $n_H$  is the Hill slope of the agonist.

154 Analysis of competitive inhibition was performed by Schild Plot according to  
 155 the following equation:

$$156 \quad \log[(EC_{50}'/EC_{50}) - 1] = \log[L] - \log K_b \quad (Equ. 3)$$

158 where  $EC_{50}'$  and  $EC_{50}$  are values in the presence and absence of antagonist (Dose  
 159 Ratio),  $[L]$  is the concentration of antagonist, and  $K_b$  is the equilibrium dissociation  
 160 constant for the antagonist receptor interaction. Further analysis was performed using  
 161 the Gaddum-Schild equation (slope = 1) as recommended by Neubig *et al*  
 162 (2003):(Neubig et al., 2003)

$$163 \quad pEC_{50} = -\log([L] + 10^{-pA_2}) - \log C \quad (Equ. 4)$$

165 where  $pEC_{50}$  is the negative logarithm of the agonist  $EC_{50}$ ,  $[L]$  is the antagonist  
 166 concentration,  $\log C$  is a constant and  $pA_2$  is the negative logarithm of the antagonist  
 167 concentration needed to double the concentration of agonist required in order to elicit  
 168 a response that is comparable to the original response in the absence of antagonist.  
 169  $pA_2$  is equal to the negative logarithm of  $K_b$  when the slope of the Schild plot is  
 170 exactly 1.

171 Kinetic parameters were determined according to the following model of a  
 172 simple bimolecular binding scheme:



175 where  $L$  is the free ligand concentration,  $R$  is receptor concentration,  $LR$  is the ligand-  
 176 receptor complex and  $k_{on}$  and  $k_{off}$  are the microscopic association and dissociation rate  
 177 constants. In a simple scheme such as this, the equilibrium dissociation constant ( $K_d$ )  
 178 is equal to the ratio of dissociation to association rate constants, such that:

$$K_d = \frac{k_{off}}{k_{on}} \quad (\text{Equ. 6})$$

181 According to a one site binding model of the type shown, the time constants for the  
 182 onset and recovery of an antagonist response can be used to estimate  $k_{+1}$  and  $k_{-1}$ :

183

$$1/\tau_{off} = k_{-1} \quad (\text{Equ. 7})$$

185 and

$$1/\tau_{on} = k_{+1}[L] + k_{-1} \quad (\text{Equ. 8})$$

187 where  $\tau_{on}$  refers to the time constant for the onset of inhibition,  $\tau_{off}$  refers to recovery  
 188 from inhibition and  $[L]$  is antagonist concentration.

189 Competition binding data were analysed by iterative curve fitting according to:

$$y = A_{\min} \frac{A_{\max} - A_{\min}}{1 + 10^{[L] - \log IC_{50}}} \quad (\text{Equ. 9})$$

191  $K_i$  values were determined from the  $IC_{50}$  values using the Cheng-Prusoff  
192 equation:

$$K_i = \frac{IC_{50}}{1 + [L]/K_d} \quad (\text{Equ. 10})$$

194 where  $K_i$  is the equilibrium dissociation constant for binding of the unlabeled ligand,  
195  $[L]$  is the concentration of labeled ligand and  $K_d$  is the equilibrium dissociation  
196 constant of the labeled ligand.

197 **Docking:** We used a template of granisetron bound to 5HTBP (PDB ID  
198 2YME); an AChBP chimera with substitutions in the binding site that mimic the 5-  
199 HT<sub>3</sub> receptor (Kesters et al., 2013). The three-dimensional structure of the  
200 hydrochloride salt of scopolamine was extracted from the Cambridge Structural  
201 Database (CSD, access code KEYSOW) and Chem3D Pro v14.0 (CambridgeSoft,  
202 Cambridge, UK) was used to construct scopolamine based on the crystal structure.  
203 The generated ligand was subsequently energy-minimised using the implemented  
204 MM2 force field. Similarly, construction of the three-dimensional structure of the  
205 protonated form of tropisetron was based on the crystal structure of *N*-methyl  
206 tropisetron (CSD access code BEGLEG), and the three-dimensional structure of SDZ-  
207 ICT 322 was based on the crystal structures of *N*-methyl tropisetron (for the indole  
208 carboxylic moiety; CSD access code BEGLEG) and scopolamine (for the tricyclic  
209 scopine moiety; CSD access code KEYSOW), followed by energy-minimisation. The  
210 binding site was defined as being within 10 Å of the centroid of the aromatic side-  
211 chain of W183, a residue that is centrally located in the binding site and is important  
212 for the binding of other 5-HT<sub>3</sub> competitive ligands. The ligands were docked into this  
213 site using GOLD Suite v5.3 (The Cambridge Crystallographic Data Centre,  
214 Cambridge, UK) with the GoldScore function and default settings. For docking,

215 scopolamine was defined as flexible, while the C-C bond between the ester group and  
216 the aromatic indole ring of SDZ-ICT322 and tropisetron was defined as rigid due to  
217 conjugation. Ten docked poses were generated for each ligand and the poses  
218 visualized with PyMol v1.7.5.0.

219

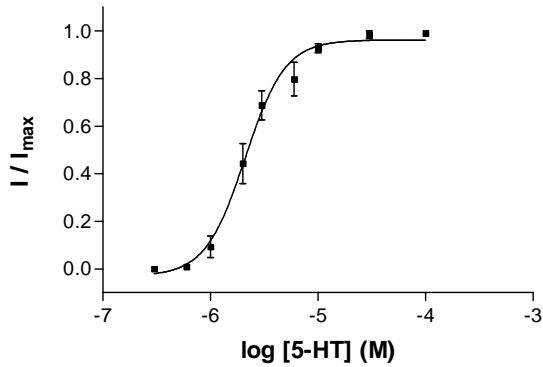
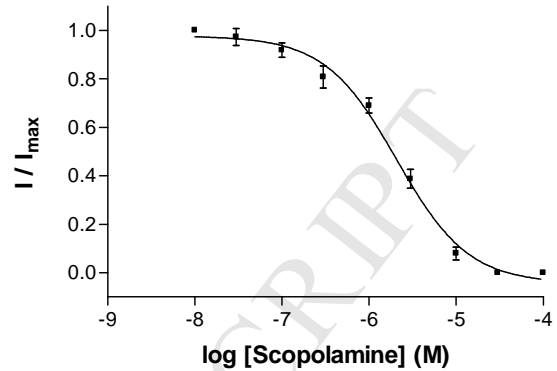
## 220 RESULTS

221 **Effects of scopolamine on 5-HT<sub>3</sub> receptor currents:** Application of 5-HT to  
222 *Xenopus* oocytes expressing the 5-HT<sub>3</sub> receptor produced concentration-dependent,  
223 rapidly activating, inward currents that slowly desensitised ( $\tau = 42 \pm 5$  seconds;  $n = 8$ )  
224 over the time-course of the applications. Plotting current amplitude against a series of  
225 5-HT concentrations allowed the data to be fitted with Equ 1 to give a pEC<sub>50</sub> of  $5.65 \pm$   
226  $0.02$  ( $EC_{50} = 2.24 \mu\text{M}$ ,  $n = 6$ ) and Hill slope of  $2.06 \pm 0.14$  (fig 2A). Agonist responses  
227 were completely inhibited by the established 5-HT<sub>3</sub> receptor-specific antagonist  
228 granisetron (100 nM, *data not shown*). Uninjected oocytes did not respond to 5-HT.

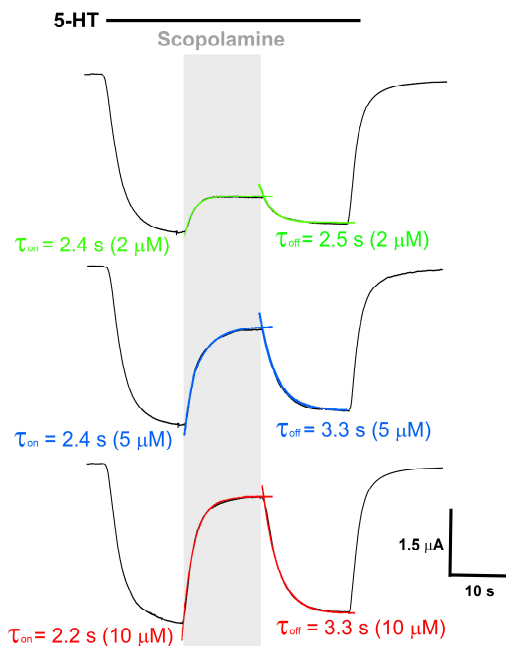
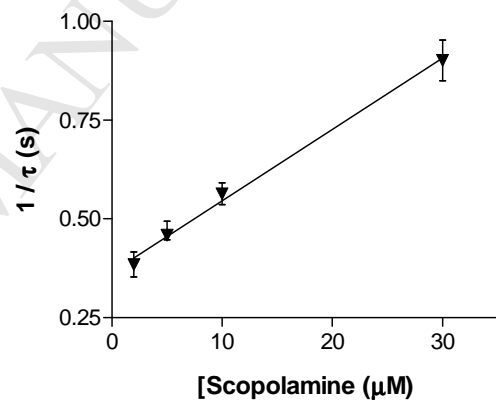
229 Application of scopolamine to oocytes expressing 5-HT<sub>3</sub> receptors did not  
230 elicit a response when applied alone, but caused a concentration-dependent inhibition  
231 of the response during a co-application of  $2 \mu\text{M}$  5-HT (fig 2). The pIC<sub>50</sub> value for  
232 scopolamine was  $5.68 \pm 0.05$  ( $IC_{50} = 2.09 \mu\text{M}$ ,  $n = 6$ ) with a Hill Slope of  $1.06 \pm 0.05$ .  
233 This gave a  $K_b$  of  $3.23 \mu\text{M}$  (Equ 2). The same concentration-dependent effect was also  
234 seen when scopolamine was applied during the 5-HT application (fig 2C). Using this  
235 protocol the onset of inhibition could be fitted with a mono-exponential function and  
236 the reciprocal plotted against antagonist concentration to yield association (slope;  $k_{\text{on}}$   
237  $= 2.6 \times 10^4 \text{ M}^{-1} \text{ s}^{-1}$ ) and dissociation (y-axis intercept;  $0.32 \text{ s}^{-1}$ ) rates that gave a  $K_d$  of  
238  $12.3 \mu\text{M}$  (fig 2D, Equ .6). Inhibition was fully reversible after 1 minute of washing  
239 and was unaltered by a 1 min scopolamine pre-application (*data not shown*).

240

241

242 **A**243 **B**

248

249 **C**250 **D**259 **Figure 2**260 The effect of scopolamine on 5-HT<sub>3</sub> receptor currents. **(A)** Concentration-response261 curve for 5-HT. **(B)** Concentration-inhibition of the 2 μM 5-HT response by co-

262 applied scopolamine. The data in 2A are normalised to the peak current response for

263 each oocyte and represented as the mean ± S.E.M. for a series of oocytes. In fig 2B,

264 inhibition by scopolamine is shown relative to the peak current response to 2 μM 5-

265 HT alone. For 5-HT curve fitting yielded a  $pEC_{50}$  of  $5.65 \pm 0.02$  ( $EC_{50} = 2.24 \mu\text{M}$ ,  $n =$   
 266 6) and Hill slope of  $2.06 \pm 0.14$ . The  $pIC_{50}$  value for scopolamine was  $5.68 \pm 0.05$   
 267 ( $IC_{50} = 2.09 \mu\text{M}$ ,  $n = 6$ ) with a Hill Slope of  $1.06 \pm 0.05$ . (C) Sample traces showing  
 268 the onset ( $\tau_{\text{on}}$ ) and recovery ( $\tau_{\text{off}}$ ) of scopolamine inhibition (*grey bar*) during a  $2 \mu\text{M}$   
 269 5-HT application (*filled bar*). (D) Onset of inhibition was well fitted by mono-  
 270 exponential functions to give  $k_{\text{obs}}$  ( $n = 17$ ). A plot of the reciprocal of these time  
 271 constants versus the scopolamine concentration showed a linear relationship where  
 272 the slope =  $k_{\text{on}}$  ( $1.61 \times 10^4 \text{ M}^{-1} \text{ s}^{-1}$ ) and the y-axis intercept =  $k_{\text{off}}$  ( $0.37 \text{ s}^{-1}$ ).

273

274 **Mechanism of scopolamine block:** Increasing concentrations of scopolamine  
 275 ( $10 \mu\text{M}$ ,  $30 \mu\text{M}$ ,  $60 \mu\text{M}$ ,  $100 \mu\text{M}$ ,  $300 \mu\text{M}$ ) caused a parallel rightward shift in the 5-  
 276 HT concentration-response curve, with no change in the maximal response (fig 3A,  
 277 table 1). A Schild plot of these results (fig 3B), yielded a gradient close to 1 ( $1.06 \pm$   
 278  $0.10$ ,  $R^2 = 0.97$ ) and a  $pA_2$  value of  $5.03 \pm 0.43$  ( $K_b = 9.33 \mu\text{M}$ ). The  $K_b$  estimate was  
 279 similar ( $2.88 \mu\text{M}$ ) if the data were fitted using a nonlinear regression method (Equ. 4)  
 280 as recommended by Neubig *et al* (2003) and Lew and Angus (1995). These data  
 281 support a competitive mechanism of action, indicating that scopolamine binds to the  
 282 orthosteric binding site. (Lew and Angus, 1995)

283

284 **Table 1**

285 Parameters derived from concentration-response curves in the presence of increasing  
 286 concentrations of scopolamine.

[Scopolamine] ( $\mu\text{M}$ )	$pEC_{50}$	$EC_{50}$ ( $\mu\text{M}$ )	$nH$	$n$
Control	$5.65 \pm 0.02$	2.24	2.1	6
10	$5.49 \pm 0.04$	3.23	2.2	4



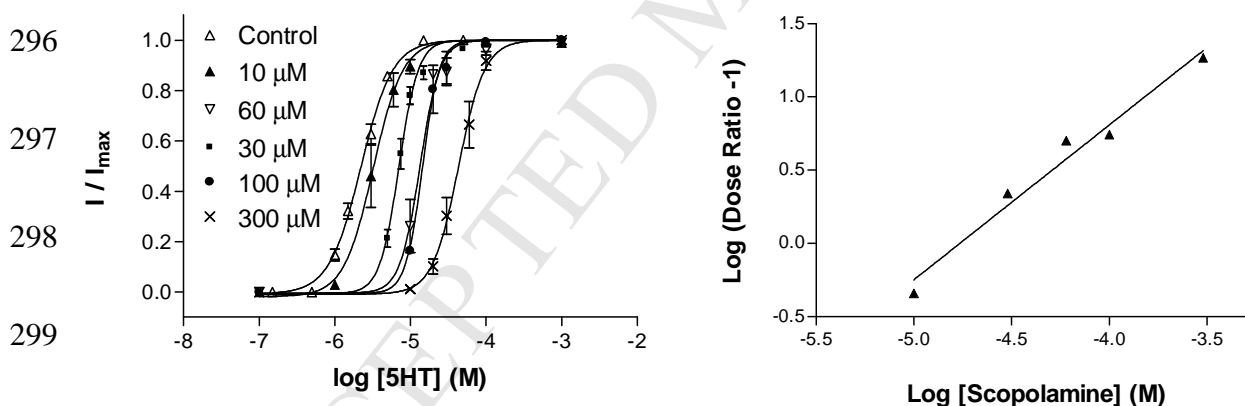
30	$5.15 \pm 0.01$	7.08	3.3	4
60	$4.87 \pm 0.03$	13.5	3.4	4
100	$4.84 \pm 0.04$	14.4	3.9	3
300	$4.36 \pm 0.03$	43.6	2.5	5

287

288 **Binding at 5-HT<sub>3</sub> and muscarinic receptors:** To further test for a  
 289 competitive binding at the 5-HT<sub>3</sub> receptor, we measured competition of unlabelled  
 290 scopolamine with [<sup>3</sup>H]granisetron, an established high-affinity competitive antagonist  
 291 at these receptors. Scopolamine displayed concentration-dependent competition with  
 292 0.6 nM [<sup>3</sup>H]granisetron ( $\sim K_d$ , fig. 4), yielding an average  $pK_i$  (Equ. 10) of  $5.17 \pm 0.24$   
 293 (fig 4;  $K_i = 6.76 \mu\text{M}$ ,  $n = 3$ ).

294

295



300

301 **Figure 3**

302 The mechanism of 5-HT<sub>3</sub> receptor inhibition by scopolamine. (A) Concentration-  
 303 response curves were performed in the absence or presence of the indicated  
 304 concentrations of scopolamine. The curves showed parallel dextral shifts with  
 305 maximal currents restored by increasing concentrations of 5-HT. Parameters derived  
 306 from these curves can be seen in table 1. (B) A Schild plot was created from the dose

307 ratios of the curves shown in 3A and fitted with Equ. 3. to yield a slope of  $1.06 \pm 0.10$   
308 ( $R^2 = 0.97$ ) and a  $pA_2$  of  $5.03 \pm 0.43$  ( $K_b$ ,  $2.88 \mu\text{M}$ ).

309

310

311 Saturation binding using radiolabelled scopolamine was also undertaken at 5-  
312  $\text{HT}_3$  receptors. Although the  $K_i$  of scopolamine was too low to accurately measure  
313 binding, the compound [ $^3\text{H}$ ]N-methylscopolamine that we used contains a permanent  
314 quaternary amine that increases its affinity at nicotinic receptors (fig. 1, Schmeller et  
315 al., 1995). However, at concentrations of up to 10 nM, no saturable binding was  
316 observed for this radioligand at 5- $\text{HT}_3$  receptors.

317 Competition of scopolamine was also measured at 5- $\text{HT}_3$  receptor by flow  
318 cytometry with a fluorescently labelled form of granisetron (G-FL, (Jack et al.,  
319 2015)). Concentration-dependent competition of G-FL with scopolamine gave an  
320 average  $pK_i$  (Equ. 11) of  $5.31 \pm 0.09$  (fig 4;  $K_i = 4.90 \mu\text{M}$ ,  $n = 8$ ). This is similar to the  
321 affinities measured using electrophysiology and radioligand binding and provides  
322 further support for a competitive mode of action.

323 In the reverse experiment, competition binding of granisetron with [ $^3\text{H}$ ]N-  
324 methylscopolamine was examined at muscarinic receptors. The  $IC_{50}$  for granisetron at  
325 muscarinic receptors was  $14.1 \pm 3.1 \mu\text{M}$  ( $n = 7$ ), yielding a  $K_i$  of  $6.5 \mu\text{M}$  (Equ. 10).

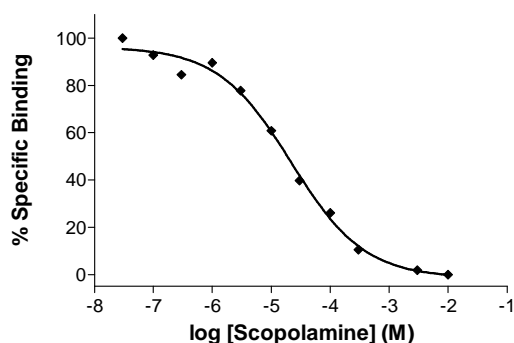
326 **Properties of atropine:** Atropine is a structurally related muscarinic  
327 antagonist (fig. 1). To test its pharmacological properties we performed measurements  
328 using electrophysiology and flow cytometry. In oocytes expressing 5- $\text{HT}_3$  receptors,  
329 atropine did not elicit a response when applied alone, but it caused concentration-  
330 dependent inhibition of the  $2 \mu\text{M}$  5-HT-evoked response with a  $pIC_{50}$  of  $5.76 \pm 0.14$   
331 ( $IC_{50} = 1.74 \mu\text{M}$ ,  $n = 5$ ) and Hill Slope of  $1.06 \pm 0.05$  (fig 5A). This yielded a  $K_b$  of

332 1.89  $\mu\text{M}$  (Equ 2). Inhibition was fully reversible after 1 minute of washing and was  
 333 unaltered by pre-application (*data not shown*).

334 Competition of G-FL and atropine was also shown by flow cytometry (fig  
 335 5B). Concentration-dependent measurements were fitted to give a  $pK_i$  (Equ 10) of  
 336  $5.10 \pm 0.16$  ( $K_i = 7.94 \mu\text{M}$ ,  $n = 5$ ).

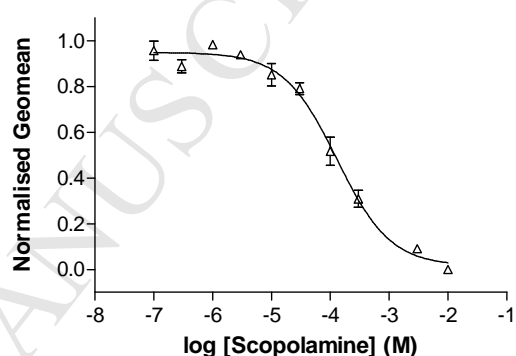
337

338 **A**



344

338 **B**



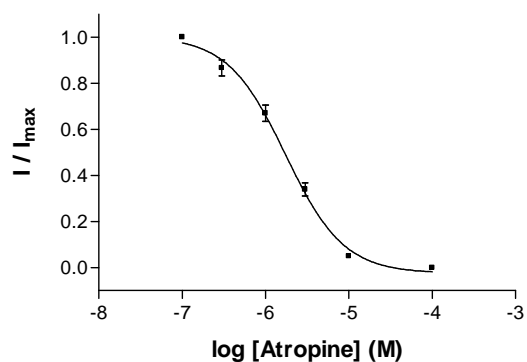
345 **Figure 4**

346 Competition of scopolamine with an established 5-HT<sub>3</sub> receptor antagonist. (A)  
 347 Radioligand binding curves for the competition of 0.6 nM [<sup>3</sup>H]granisetron and  
 348 varying concentrations of scopolamine at crude membrane extracts of 5-HT<sub>3</sub> receptors  
 349 from stably expressing HEK 293 cells. Data was normalised to [<sup>3</sup>H]granisetron  
 350 binding in the absence of antagonist and fitted with Equ. 10. The curve is  
 351 representative of 3 similar experiments, which gave an average  $pK_i$  of  $5.17 \pm 0.24$  ( $K_i$   
 352 =  $6.76 \mu\text{M}$ ,  $n = 3$ ). (B) Flow cytometry, showing the competition of 10 nM G-FL (a  
 353 fluorescent derivative of granisetron; Jack et al., 2015) and varying concentrations of  
 354 scopolamine at 5-HT<sub>3</sub> receptors expressed on the surface of live HEK 293 cells. The  
 355 average  $pK_i$  of these experiments was similar to values from radioligand competition  
 356 ( $5.31 \pm 0.09$ ,  $K_i = 4.90 \mu\text{M}$ ,  $n = 8$ ).

357

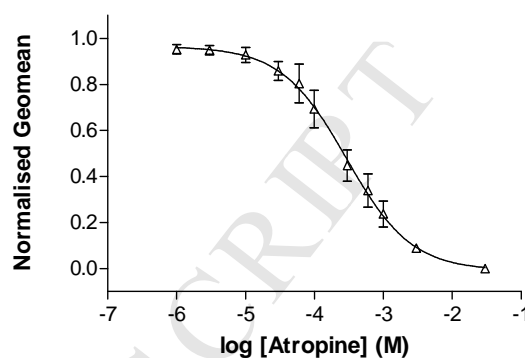
358

359 A



363

360 B

364 **Figure 5**

365 Effects of atropine on the electrophysiological responses to 5-HT and binding of G-  
 366 FL. (A) Concentration-inhibition of the 2  $\mu$ M 5-HT response by co-applied atropine.

367 For each oocyte the responses in the presence of antagonist are normalised to the peak  
 368 current response to 5-HT alone and data represented as the mean  $\pm$  S.E.M. for a series  
 369 of oocytes. Curve fitting yielded a  $pIC_{50}$  of  $5.76 \pm 0.14$  ( $IC_{50} = 1.74 \mu$ M,  $n = 5$ ) and

370 Hill Slope of  $1.06 \pm 0.05$ . (B) Flow cytometry, showing the competition of 10 nM G-  
 371 FL (a fluorescent derivative of granisetron; Jack et al., 2015) and varying

372 concentrations of atropine at 5-HT<sub>3</sub> receptors expressed on the surface of live HEK  
 373 293 cells. The affinity ( $pK_i = 5.10 \pm 0.16$ ,  $K_i = 7.94 \mu$ M,  $n = 5$ ) of atropine calculated

374 from these experiments was similar to that measured using electrophysiology.  
 375

376

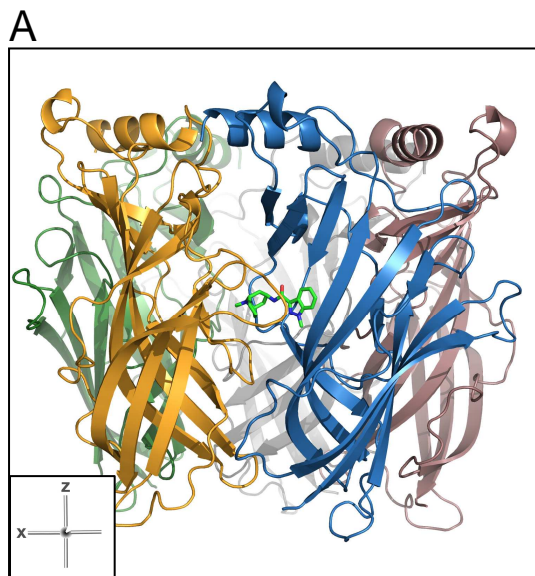
377 **Docking studies:** Based upon the evidence that scopolamine binds at the  
 378 orthosteric binding site we used a bio-informatics approach to probe possible ligand  
 379 orientations and try to understand why the affinity of scopolamine was lower than  
 380 other established 5-HT<sub>3</sub> receptor antagonists. To this end we chose a crystal structure

381 of a 5-HT<sub>3</sub> receptor-AChBP chimera (termed 5HTBP) complexed with granisetron  
382 (PDB ID: 2YME) as a binding site model (fig 6A, Kesters et al., 2013). For the  
383 purpose of validation we first removed granisetron from the template and re-docked  
384 both this ligand and the closely related 5-HT<sub>3</sub> receptor antagonist, tropisetron, into the  
385 binding site template. The proposed ligand orientations of these two antagonists were  
386 almost identical to the binding pose from the crystal structure 2YME. This is  
387 illustrated in fig. 6B where tropisetron is shown with its bicyclic moiety located  
388 between the aromatic side chains of W90, W183 and Y234 and the flat indole ring is  
389 sandwiched between loop C and R92 from loop D.

390 Following from our docking with established 5-HT<sub>3</sub> antagonists, we  
391 performed docking with scopolamine. This yielded a docked pose cluster (fig. 6C)  
392 that placed the scopine head of scopolamine at the same location as the azabicyclic  
393 rings of granisetron and tropisetron, but owing to the flexibility of scopolamine and  
394 the steric restraints imposed by the tight binding cavity, the hydroxyl of the carbonyl  
395 linker was extended into a pocket at the rear of the binding site, displacing the  
396 aromatic ring by ~ 3 Å towards the principal binding interface (fig 6D).

397 SDZ-ICT 322 (fig. 1), is a competitive, highly potent 5-HT<sub>3</sub> receptor  
398 antagonist that contains key structural elements of both scopolamine and high affinity  
399 5-HT<sub>3</sub> receptor antagonists such as granisetron and tropisetron (Blum et al., 1992); it  
400 has the same tricyclic scopine moiety as scopolamine, which is rigidly linked to the  
401 flat heteroaromatic group (indole) found in granisetron and tropisetron. Docking of  
402 SDZ-ICT 322 into the 5-HT<sub>3</sub> receptor binding site predicted an orientation similar to  
403 granisetron and tropisetron, with its aromatic indole group close to the side chain of  
404 R92 from loop D and the scopine tricycle pointing towards the β-sheets of the  
405 principal face, surrounded by the aromatic rings of W90, W183 and Y234 (fig. 6E).

406



407

408

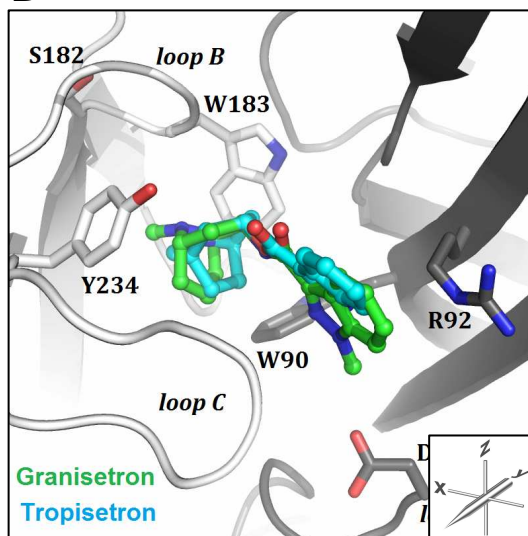
409

410

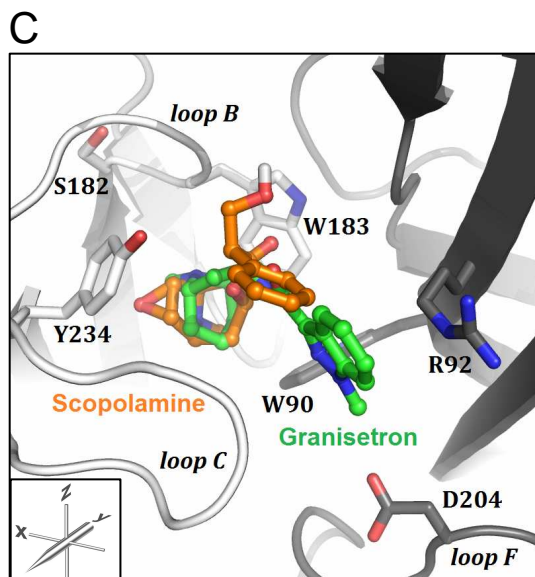
411

412

413

**B**

414



415

416

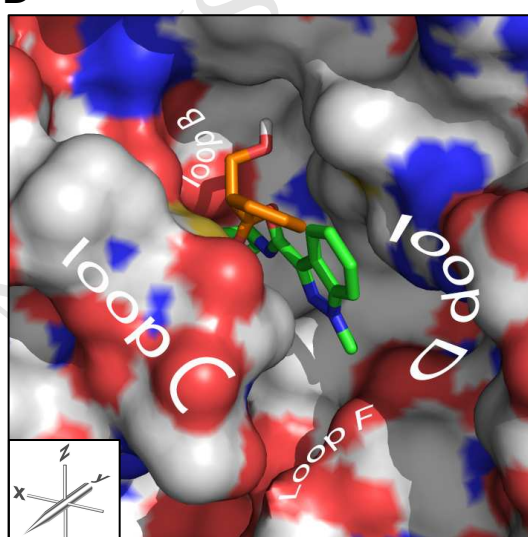
417

418

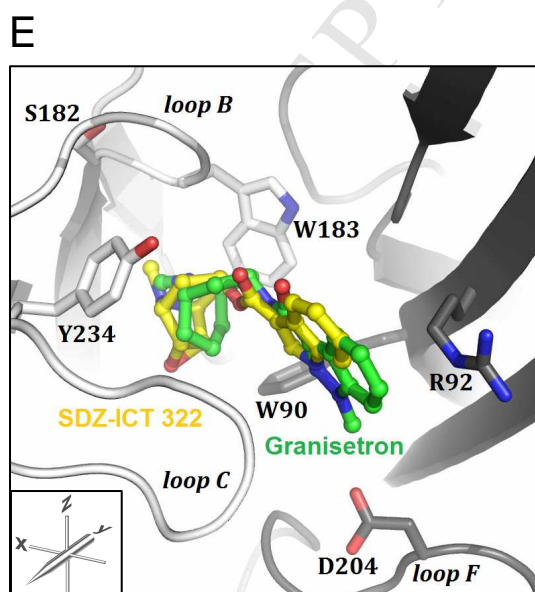
419

420

421

**D**

422



423

424

425

426

427

428

429

430

431 **Figure 6**

432 representative examples of 5-HT<sub>3</sub> receptor antagonists (ball-and-stick representation)  
433 docked into a 5-HT<sub>3</sub> receptor orthosteric binding site model (PDB ID: 2YME; a co-  
434 crystal of granisetron bound to a mutant AChBP that contains residues from the 5-HT<sub>3</sub>  
435 receptor binding site (termed 5HTBP; Kesters et al., 2013) and important binding site  
436 residues (stick representation). Principle face (left-hand side, light grey),  
437 complementary face (right-hand side, dark grey). **(A)** 2YME from the side (y-axis)  
438 showing the location of granisetron (green) in the orthosteric binding site at the  
439 interface of two adjacent subunits. **(B)** Proposed binding pose for tropisetron (blue)  
440 overlaying granisetron (green) from the co-crystal structure 2YME. **(C)** The proposed  
441 binding pose for scopolamine (orange) showing its orientation in the 5-HT<sub>3</sub> binding  
442 site. **(D)** A surface representation of 5HTBP bound with granisetron and an overlay of  
443 docked scopolamine showing the hydroxyl of the carbonyl linker that, owing to steric  
444 constraints, is located within a cavity at the rear of the binding site. It can be seen that  
445 while the scopine head of scopolamine (orange) is at the same location as the  
446 azabicyclic rings of granisetron (green), the steric bulk, flexibility and presence of a  
447 hydroxyl in the linker region results in the aromatic ring being orientated away from  
448 loops D and F. **(D)** In contrast, the proposed binding pose for SDZ-ICT 322 (yellow)  
449 is more similar to that of granisetron. For chemical structures of the described ligands  
450 see fig. 1.

451

452 **DISCUSSION**

453 This study describes the effects of scopolamine and atropine on human 5-HT<sub>3</sub>  
454 receptors. Both compounds were antagonists with  $\mu\text{M}$  potencies. For scopolamine,  
455 binding at the orthosteric site was demonstrated by Schild analysis and competition

456 with the 5-HT<sub>3</sub> receptor antagonists [<sup>3</sup>H]granisetron and G-FL. *In silico* docking  
457 predicted that molecular features of the carbonyl linker of scopolamine may alter its  
458 orientation within the binding site and could account for the lower potency when  
459 compared to established 5-HT<sub>3</sub> receptor antagonists. Evidence for this is discussed in  
460 more detail below.

461 The observation that scopolamine competitively inhibits 5-HT<sub>3</sub> receptor  
462 responses was anticipated as it has structural similarities with other 5-HT<sub>3</sub> receptor  
463 antagonists (fig 1) and ligand promiscuity at 5-HT<sub>3</sub> receptors has been reported  
464 elsewhere. For example, epibatidine and tropisetron are high affinity agonists of  $\alpha 7$   
465 nACh and high affinity antagonists of 5-HT<sub>3</sub> receptors. Similarly, 5-HT<sub>3</sub> receptors  
466 also have lower affinity competitive interactions with dopamine, acetylcholine,  
467 nicotine, *d*-tubocurarine, chloroquine, varenecline and strychnine, as well as allosteric  
468 modulators such as anaesthetics, alcohols, steroids and terpenoids and the non-  
469 competitive antagonists picrotoxin, ginkgolides and mefloquine (Thompson and  
470 Lummis, 2008; Thompson and Lummis, 2013; Thompson et al., 2014). It is perhaps  
471 more surprising that the affinities of scopolamine and atropine were not higher given  
472 their structural similarities to 5-HT<sub>3</sub> receptor antagonists that bind with nM affinities.  
473 However, the lower affinities are likely to result from both scopolamine and atropine  
474 having an aromatic ring that is not directly attached to the ester moiety that forms the  
475 link with the bicyclic amine, a bond that is common to all 5-HT<sub>3</sub> receptor antagonists  
476 (Thompson, 2013). The direct conjugation of the carbonyl (ester or amide) group with  
477 the aromatic ring provides 5-HT<sub>3</sub> receptor antagonists with planarity and rigidity that  
478 is crucial for potent inhibition and high-affinity binding (Hibert, 1994). Instead,  
479 scopolamine and atropine have linkers that contain a tetrahedral carbon that carries a  
480 polar hydroxymethyl substituent (fig 1). The importance of this region is highlighted



481 by SDZ-ICT 322, a ligand that is also a high affinity 5-HT<sub>3</sub> receptor antagonist ( $pA_2 =$   
482 10.6 in isolated rabbit vagus nerve,  $pK_d = 9.2$  in N1E cells) but has the same scopolamine  
483 tricyclic moiety as scopolamine directly linked to the aromatic indole ring (Blum et  
484 al., 1992). This hypothesis is further supported by the low affinity of atropine which  
485 contains the same tetrahedral carbon, while the close analogue tropane benzoate, with  
486 a carbonyl linker, has high affinity at 5-HT<sub>3</sub> receptors (63 nM; Fozard 1989). We also  
487 found that the potent 5-HT<sub>3</sub> receptor antagonist, granisetron, binds with a micromolar  
488 affinity at muscarinic receptors, suggesting that while general conformations of these  
489 ligands enable them to share common binding sites at both receptors, the linkers are  
490 likely to confer the key structural elements that drive receptor selectivity.

491 To find further evidence for the importance of this linker region, we performed  
492 docking into a homologue of the 5-HT<sub>3</sub> receptor that has been co-crystallised with the  
493 antagonist granisetron in its binding site (Kesters et al., 2013). The predicted binding  
494 pose for the high affinity antagonist SDZ-ICT 322 was similar to the orientations of  
495 granisetron and tropisetron ligands in 5HTBP and AChBP co-crystal structures (fig  
496 6E), which was anticipated given the similarity in their structures (fig. 1) and affinities  
497 (Hibbs et al., 2009; Kesters et al., 2013). However, in scopolamine the tri-substituted  
498 tetrahedral carbon between the scopolamine tricyclic moiety and the aromatic phenyl ring  
499 leads to a kink in the molecular structure, unlike the high-affinity 5-HT<sub>3</sub> receptor  
500 which are planar. In scopolamine this linker also contains a hydroxyl group. The  
501 docking results lead us to speculate that the substituted tetrahedral carbon in  
502 scopolamine creates increased bulk and ligand flexibility, while the polar hydroxyl  
503 group is sterically restricted and occupies a cavity in the rear of the binding site. If  
504 these predictions are correct, the differences in the linker region orientate scopolamine  
505 away from residues in binding loops D and F (fig 6D), and the ligand no longer

506 engages with residues that are essential for high affinity binding (Thompson et al.,  
507 2005; Thompson et al., 2006).

508 Scopolamine is generally regarded as a non-selective muscarinic receptor  
509 antagonist with an affinity  $\leq 1$  nM. At higher concentrations it also blocks nicotinic  
510 acetylcholine receptors ( $IC_{50} = 928$   $\mu$ M) and increases the expression of  $\alpha 7$  nACh  
511 receptors (Schmeller et al., 1995; Falsafi et al., 2012). When using scopolamine for  
512 the prevention of motion sickness in humans, blood concentrations following  
513 transdermal and combined oral administration have been reported to peak at  $\sim 0.37$  ng  
514  $ml^{-1}$  within an hour (Nachum et al., 2001). Elsewhere, higher plasma concentrations  
515 of  $2.9$  ng  $ml^{-1}$  are reported following intravenous administration ( $0.4$  mg) to healthy  
516 volunteers (Putchá et al., 1989). Both of these values are significantly lower than the  
517 concentrations that affect 5-HT<sub>3</sub> receptors and it is unlikely that these receptors would  
518 be inhibited. However, when scopolamine is used to induce cognitive dysfunction in  
519 rodents, intraperitoneal or sub-cutaneous injections of up to  $2$  mg  $kg^{-1}$  are used  
520 (Klinkenberg and Blokland, 2010). As a weight per volume this is the equivalent of  
521  $\sim 1$   $\mu$ M which is close to the  $IC_{50}$  at 5-HT<sub>3</sub> receptors. For centrally administered  
522 scopolamine the focal concentrations at the site of administration can be as high as  
523  $140$   $\mu$ g  $\mu l^{-1}$  ( $460$   $\mu$ M), a concentration that is far in excess of its  $IC_{50}$  at 5-HT<sub>3</sub>  
524 receptors and would cause complete inhibition (Klinkenberg and Blokland, 2010).

525 The amygdala and hippocampus are of critical importance in implicit and  
526 explicit memory, and this function is mediated via actions of both cholinergic and  
527 serotonergic pathways. As scopolamine blocks muscarinic receptors with high affinity  
528 it is used to induce cognitive dysfunction, but it is also known that 5-HT<sub>3</sub> receptor  
529 antagonists alleviate these symptoms. Long-term potentiation (LTP, the neural  
530 mechanism through which memory is formed) in the amygdala and hippocampus is

531 inhibited by 5-HT<sub>3</sub> receptor agonists and promoted by antagonists (Staubli and Xu,  
532 1995). These effects are probably mediated via actions on the GABA-ergic synaptic  
533 activity of interneurons, but may also result from activities at 5-HT<sub>3</sub> receptors that are  
534 present outside of the hippocampus and would also be blocked by systemically  
535 administered 5-HT<sub>3</sub> antagonists. If sufficiently high concentrations of scopolamine  
536 were centrally administered we might expect a similar block of 5-HT<sub>3</sub> receptors which  
537 could complicate the interpretation of its physiological effects. Pre-administering 5-  
538 HT<sub>3</sub> antagonists to alleviate cognitive dysfunction might further complicate these  
539 studies as their higher affinities and slower elimination from the body would prevent  
540 scopolamine binding at 5-HT<sub>3</sub> receptors (Putchá et al., 1989). As mood disorders such  
541 as anxiety and depression are also mediated by both cholinergic and serotonergic  
542 pathways, the interpretation of scopolamine effects on these might be similarly  
543 affected (Bétry et al., 2011).

544 In summary, we provide the first reported evidence that the drug scopolamine  
545 inhibits the function of homomeric 5-HT<sub>3</sub> receptors via a competitive mode of action,  
546 and suggest that the bond that links the kinked and more flexible structure of  
547 scopolamine is responsible for the lower affinity when compared with other typically  
548 flat and rigid 5-HT<sub>3</sub> receptor antagonists. Because the concentration of centrally  
549 administered scopolamine can exceed the concentration that inhibits 5-HT<sub>3</sub> receptors,  
550 it is likely that these receptors would be inhibited under this experimental paradigm,  
551 and could influence LTP. Given this finding we believe that the potential effects at 5-  
552 HT<sub>3</sub> receptors should be considered before centrally administering high  
553 concentrations of this compound.

554

555

556 **ACKNOWLEDGMENTS**

557

558 Our thanks are given to John Peters (University of Dundee) for the 5-HT3A subunit.

559 ML thanks the Swiss National Science Foundation for financial support (SNSF-

560 professorship PP00P2\_123536 and PP00P2\_146321). AJT thanks the British Heart

561 Foundation for financial support (PG/13/39/30293).

562

563 There are no conflicts of interest arising from this work.

564

565

566 **AUTHORSHIP CONTRIBUTIONS**

567

568 *Participated in research design:* AJT

569 *Conducted experiments:* AJT

570 *Contributed reagents or analytical tools:* -

571 *Performed data analysis:* AJT, ML

572 *Wrote or contributed to the writing of the manuscript:* AJT, ML

573

574

575

576

577 **REFERENCES**

578

579 Barnes JM, Costall B, Coughlan J, Domeney AM, Gerrard PA, Kelly ME, Naylor RJ,

580 Onaivi ES, Tomkins DM and Tyers MB (1990) The Effects of Ondansetron, a

- 581 5-HT<sub>3</sub> Receptor Antagonist, on Cognition in Rodents and Primates.  
582 *Pharmacol Biochem Behavior* **35**:955-962.
- 583 Bartolomeo AC, Morris H, Buccafusco JJ, Kille N, Rosenzweig-Lipson S, Husbands  
584 MG, Sabb AL, Abou-Gharbia M, Moyer JA and Boast CA (2000) The  
585 preclinical pharmacological profile of WAY-132983, a potent M1 preferring  
586 agonist. *J Pharmacol Exp Ther* **292**:584-596.
- 587 Bartus RT (2000) On neurodegenerative diseases, models, and treatment strategies:  
588 lessons learned and lessons forgotten a generation following the cholinergic  
589 hypothesis. *Exp Neurol* **163**:495-529.
- 590 Bétry, C., Etiévant, A., Oosterhof, C., Ebert, B., Sanchez C., N., H., 2011. Role of 5-HT<sub>3</sub>  
591 Receptors in the Antidepressant Response. *Pharmaceuticals* **4**; 603-629.
- 592 Blin O, Audebert C, Pitel S, Kaladjian A, Casse-Perrot C, Zaim M, Micallef J, Tisne-  
593 Versailles J, Sokoloff P, Chopin P and Marien M (2009) Effects of  
594 dimethylaminoethanol pyroglutamate (DMAE p-Glu) against memory deficits  
595 induced by scopolamine: evidence from preclinical and clinical studies.  
596 *Psychopharmacology (Berl)* **207**:201-212.
- 597 Blum E, Buchheit KH, Buescher HH, Gamse R, Kloepfner E, Meigel H,  
598 Papageorgiou C, Waelchli R and Revesz L (1992) Design and Synthesis of  
599 Novel Ligands for the 5-HT<sub>3</sub> and the 5-HT<sub>4</sub> Receptor. *Bioorg Med Chem Lett*  
600 **2**:461-466.
- 601 Brown, A. M., Hope, A. G., Lambert, J. J., Peters, J. A., 1998. Ion permeation and  
602 conduction in a human recombinant 5-HT<sub>3</sub> receptor subunit (h5-HT3A). *J*  
603 *Physiol* **507**: 653-665.

- 604 Carli M, Luschi R and Samanin R (1997) Dose-related impairment of spatial learning  
605 by intrahippocampal scopolamine: Antagonism by ondansetron, a 5-HT<sub>3</sub>  
606 receptor antagonist. *Behav Brain Res* **82**:185-194.
- 607 Chugh Y, Saha N, Sankaranarayanan A and Datta H (1991) Enhancement of Memory  
608 Retrieval and Attenuation of Scopolamine-Induced Amnesia Following  
609 Administration of 5-HT<sub>3</sub> Antagonist ICS-205-930. *Pharmacol Toxicol* **69**:105-  
610 106.
- 611 Falsafi SK, Deli A, Hoger H, Pollak A and Lubec G (2012) Scopolamine  
612 Administration Modulates Muscarinic, Nicotinic and NMDA Receptor  
613 Systems. *PloS one* **7**.
- 614 Fozard JR, (1989) The Development and Early Clinical Evaluation of Selective 5-  
615 HT<sub>3</sub> Receptor Antagonists. in *The Peripheral Actions of 5-  
616 Hydroxytryptamine*, Fozard JR. (Ed.), Oxford Medical Publications, Oxford,  
617 354-376.
- 618 Goldin LR (1992) Maintenance of *Xenopus laevis* and Oocyte Injection. In *Methods  
619 in Enzymology* 207, Bernardo, R. and Iverson, L. E. (Eds.), Academic Press,  
620 New York. **207**:267-279.
- 621 Gulyas AI, Acsady L and Freund TF (1999) Structural basis of the cholinergic and  
622 serotonergic modulation of GABAergic neurons in the hippocampus.  
623 *Neurochem Int* **34**:359-372.
- 624 Hassaine G, Deluz C, Grasso L, Wyss R, Tol MB, Hovius R, Graff A, Stahlberg H,  
625 Tomizaki T, Desmyter A, Moreau C, Li XD, Poitevin F, Vogel H and Nury H  
626 (2014) X-ray structure of the mouse serotonin 5-HT<sub>3</sub> receptor. *Nature*  
627 **512**:276-281.

- 628 Hibbs RE, Sulzenbacher G, Shi J, Talley TT, Conrod S, Kem WR, Taylor P, Marchot  
629 P and Bourne Y (2009) Structural determinants for interaction of partial  
630 agonists with acetylcholine binding protein and neuronal  $\alpha 7$  nicotinic  
631 acetylcholine receptor. *Embo J* **28**:3040-3051.
- 632 Hibert M (1994) Molecular modelling studies of the 5-HT<sub>3</sub> receptor antagonist  
633 recognition site. In 5-Hydroxytryptamine-3 Receptor Antagonists, King FD,  
634 Jones BJ, Sanger GJ (Eds.), CRC Press: 1994:45-66.
- 635 Jack T, Simonin J, Ruepp MD, Thompson AJ, Gertsch J and Lochner M (2015)  
636 Characterizing new fluorescent tools for studying 5-HT<sub>3</sub> receptor  
637 pharmacology. *Neuropharmacol* **90**:63-73.
- 638 Kesters D, Thompson AJ, Brams M, van Elk R, Spurny R, Geitmann M, Villalgorido  
639 JM, Guskov A, Danielson UH, Lummis SC, Smit AB and Ulens C (2013)  
640 Structural basis of ligand recognition in 5-HT<sub>3</sub> receptors. *EMBO reports*  
641 **14**:49-56.
- 642 Klinkenberg I and Blokland A (2010) The validity of scopolamine as a  
643 pharmacological model for cognitive impairment: A review of animal  
644 behavioral studies. *Neurosci Biobehav Rev* **34**:1307-1350.
- 645 Leff P and Dougall IG (1993) Further concerns over Cheng-Prusoff analysis. *Trends*  
646 *Pharmacol Sci* **14**:110-112.
- 647 Lew MJ and Angus JA (1995) Analysis of competitive agonist-antagonist interactions  
648 by nonlinear regression. *Trends Pharmacol Sci* **16**:328-337.
- 649 Liem-Moolenaar M, de Boer P, Timmers M, Schoemaker RC, van Hasselt JG,  
650 Schmidt S and van Gerven JM (2011) Pharmacokinetic-pharmacodynamic  
651 relationships of central nervous system effects of scopolamine in healthy  
652 subjects. *Br J Clin Pharmacol* **71**:886-898.

- 653 Lochner M and Thompson AJ (2015) A review of fluorescent ligands for studying 5-  
654 HT<sub>3</sub> receptors. *Neuropharmacology*. In Press.
- 655 Lowry OH, Rosebrough NJ, Farr AL and Randall RJ (1951) Protein measurement  
656 with the Folin phenol reagent. *J Biol Chem* **193**:265-275.
- 657 Nachum Z, Shahal B, Shupak A, Spitzer O, Gonen A, Beiran I, Lavon H, Eynan M,  
658 Dachir S and Levy A (2001) Scopolamine bioavailability in combined oral and  
659 transdermal delivery. *J Pharmacol Exp Ther* **296**:121-123.
- 660 Neubig RR, Spedding M, Kenakin T and Christopoulos A (2003) International Union  
661 of Pharmacology Committee on Receptor Nomenclature and Drug  
662 Classification. XXXVIII. Update on terms and symbols in quantitative  
663 pharmacology. *Pharmacol Rev* **55**:597-606.
- 664 Peters JA, Cooper MA, Carland JE, Livesey MR, Hales TG and Lambert JJ (2010)  
665 Novel structural determinants of single channel conductance and ion  
666 selectivity in 5-hydroxytryptamine type 3 and nicotinic acetylcholine  
667 receptors. *J Physiol* **588**:587-596.
- 668 Putcha L, Cintron NM, Tsui J, Vanderploeg JM and Kramer WG (1989)  
669 Pharmacokinetics and Oral Bioavailability of Scopolamine in Normal  
670 Subjects. *Pharmaceut Res* **6**:481-485.
- 671 Schmeller T, Sporer F, Sauerwein M and Wink M (1995) Binding of Tropane  
672 Alkaloids to Nicotinic and Muscarinic Acetylcholine Receptors. *Pharmazie*  
673 **50**:493-495.
- 674 Seyedabadi M, Fakhfouri G, Ramezani V, Mehr SE and Rahimian R (2014) The role  
675 of serotonin in memory: interactions with neurotransmitters and downstream  
676 signaling. *Exp Brain Res* **232**:723-738.



- 677 Staubli U and Xu FB (1995) Effects of 5-HT<sub>3</sub> receptor antagonism on hippocampal  
678 theta rhythm, memory, and LTP induction in the freely moving rat. *J Neurosci*  
679 **15**:2445-2452.
- 680 Thompson AJ (2013) Recent developments in 5-HT<sub>3</sub> receptor pharmacology. *Trends*  
681 *Pharmacol Sci* **34**:100-109.
- 682 Thompson AJ, Lester HA and Lummis SCRL (2008) The Structural Basis of Function  
683 in Cys-loop Receptors. *Quart Rev Biophys*: **43**: 449-499
- 684 Thompson AJ and Lummis SC (2008) Antimalarial drugs inhibit human 5-HT<sub>3</sub> and  
685 GABA<sub>A</sub> but not GABA<sub>C</sub> receptors. *Br J Pharmacol* **153**:1686-1696.
- 686 Thompson AJ and Lummis SC (2013) Discriminating between 5-HT<sub>3A</sub> and 5-HT<sub>3AB</sub>  
687 receptors. *Br J Pharmacol* **169**:736-747.
- 688 Thompson AJ and Lummis SCR (2007) The 5-HT<sub>3</sub> Receptor as a Therapeutic Target.  
689 *Expert Opin Ther Targ* **11**:527-540.
- 690 Thompson AJ, Padgett CL and Lummis SC (2006) Mutagenesis and molecular  
691 modeling reveal the importance of the 5-HT<sub>3</sub> receptor F-loop. *J Biol Chem*  
692 **281**:16576-16582.
- 693 Thompson AJ, Price KL, Reeves DC, Chan SL, Chau PL and Lummis SC (2005)  
694 Locating an antagonist in the 5-HT<sub>3</sub> receptor binding site using modeling and  
695 radioligand binding. *J Biol Chem* **280**:20476-20482.
- 696 Thompson AJ, Verheij MHP, Verbeek J, Windhorst AD, de Esch IJP and Lummis  
697 SCR (2014) The binding characteristics and orientation of a novel radioligand  
698 with distinct properties at 5-HT<sub>3A</sub> and 5-HT<sub>3AB</sub> receptors. *Neuropharmacol*  
699 **86**:378-388.
- 700 Walstab J, Rappold G and Niesler B (2010) 5-HT<sub>3</sub> receptors: role in disease and target  
701 of drugs. *Pharmacol Ther* **128**:146-169.

- 702 Williams, M. J., Adinoff, B., 2008. The role of acetylcholine in cocaine addiction.  
703           Neuropsychopharmacology **33**: 1779-1797.

ACCEPTED MANUSCRIPT

- Muscarinic ligands scopolamine and atropine also have micromolar affinity at 5-HT<sub>3</sub> receptors.
- The 5-HT<sub>3</sub> receptor ligand granisetron also has micromolar affinity at muscarinic receptors
- Scopolamine has a tetrahedral carbon linker that is responsible for its lower affinity at 5-HT<sub>3</sub> receptors.
- Scopolamine is used as a preclinical model for inducing cognitive dysfunction.
- Use of high concentrations may inhibit 5-HT<sub>3</sub> receptors and complicate analysis.